

# Single Gaussian temporal pulse modulated controlled-Z gate of neutral atoms under symmetrically optical pumping

X. X. Li,<sup>1</sup> X. Q. Shao,<sup>1,2,\*</sup> and Weibin Li<sup>3,†</sup>

<sup>1</sup>*Center for Quantum Sciences and School of Physics, Northeast Normal University, Changchun 130024, China*

<sup>2</sup>*Center for Advanced Optoelectronic Functional Materials Research, and Key Laboratory for UV Light-Emitting Materials and Technology of Ministry of Education, Northeast Normal University, Changchun 130024, China*

<sup>3</sup>*School of Physics and Astronomy, The University of Nottingham, Nottingham NG7 2RD, United Kingdom*

We propose an experimentally feasible protocol for implementing the standard controlled-Z gate of neutral atoms through a symmetrical two-photon excitation process via the second resonance line,  $6P$  in  $^{87}\text{Rb}$ , with a single-Gaussian-temporal-modulation-coupling of ground state and intermediate state. For qubit states that encoded on the alkali clock states, the dynamics of system depend on different adiabatic paths modulated by Gaussian pulses, which accumulates a phase factor of  $\pi$  on logic qubit state  $|11\rangle$  alone at the end of the operation. The Gaussian pulse takes the simple form of  $\Omega_0 \exp[-(t - 2T)^2/T^2]$ , and the corresponding optimal parameters can be easily determined by direct use of numerical integration. On the premise of considering only spontaneous emission, the gate fidelity can achieve 99.78% with the operation time less than 1  $\mu\text{s}$ . Furthermore, we discuss in detail the impact of other sources of errors on the fidelity of logic gate and find that the use of adiabatic pulse makes the gate less sensitive to the Doppler effect and laser intensity fluctuation. By selecting suitable optical traps, the predicted fidelity of the gate can reach about 98.4% after correcting the measurement error. Compared with the existing schemes, we achieve a higher fidelity quantum logic gate through a simpler Gaussian driving field, which may be helpful to the experimental implementation of quantum computation and quantum simulation in the neutral-atoms system.

## I. INTRODUCTION

The neutral atoms are promising candidates for quantum computing due to their long coherence time for ground-state atoms and remarkable features for highly excited Rydberg atoms, e.g. strong and long-range interactions, long lifetime, and giant polarizability [1, 2]. According to the frequency range of the external driving field, the resulting long-range resonant (Förster) and off-resonant dipolar (van der Waals) interactions can give rise to Rydberg blockade effect [3–7], Rydberg facilitation (or antiblockade) dynamics [8–11], and Rydberg dressing mechanism [12–16] which constitute the basic principle for performing most quantum computing and quantum simulation tasks in neutral-atom system [17–51]. Nevertheless, it should be worth emphasizing that although the above three mechanisms have their own advantages for the realization of neutral atomic logic gates in theory, the characteristic of Rydberg blockade makes it stand out in experimental implementation since the fidelity of such schemes is independent of the first-order large blockade shift [52–65].

The ideas of using strong Rydberg dipole-blockade interactions for implementing two-qubit quantum gates based on individual Rydberg atoms and mesoscopic atomic ensembles were proposed by Jaksch *et al.* and Lukin *et al.* [18, 19], respectively, where the  $\pi$ - $2\pi$ - $\pi$  pulse sequence designed by them has become a conventional means for the subsequent experimental study of neutral-atom systems [53–58]. Recently, Levine *et al.* improve the traditional gate protocol by selecting a specific detuning parameter of laser light, and the two-

qubit controlled-phase gate is implemented in a faster way after two global pulses [60, 63]. In addition, compared with the constant-amplitude pulses, the temporal modulation of the laser field is more helpful to avoid unwanted transitions of quantum states and then suppresses the population leakage error [61, 65–69]. Very recently in experiment, Fu *et al.* have achieved the  $C_z$  gate with fidelity  $\mathcal{F} = 0.980(7)$  after correcting the state preparation and measurement (SPAM) errors using the single-modulated-pulse off-resonant modulated driving (SORMD) [64].

In fact, as a well-known time-dependent pulse modulation technology, the adiabatic techniques [70], such as stimulated Raman adiabatic passage (STIRAP) and adiabatic rapid passage (ARP), have long been widely applied to neutral-atom system within the Rydberg blockade region to improve the robustness against the fluctuation of parameter and reduce the requirement of the strong Rydberg interactions [66, 71–82]. The types of phase accumulation during adiabatic evolution can be roughly divided into geometric phases [71, 77, 78] and dynamic phases [73, 80]. Early scheme put forward by Møller *et al.* [71] successfully acquired a geometric phase by applying two STIRAP pulse in sequence under Rydberg blockade, and then Bhaktavatsala *et al.* modified the scheme into an intermediate Rydberg interaction regime with two STIRAP pulses applied simultaneously [77]. However, the geometric phase acquired is strongly dependent on the way the relative phase is modulated, which usually requires a longer evolution time in comparison with the dynamic one. To solve this problem, Saffman *et al.* designed a “STIRAP-inspired”  $C_z$  gate with a dynamically accumulated phase via globally optimized pulses shape. This gate can reach a high fidelity  $\mathcal{F} = 0.997$  within 1  $\mu\text{s}$  for cesium atoms in the absence of errors arising from laser noise [80, 83]. Nevertheless, as the author pointed out in the article, their scheme has higher sensitivity to in-

\* [shaoxq644@nenu.edu.cn](mailto:shaoxq644@nenu.edu.cn)

† [weibin.Li@nottingham.ac.uk](mailto:weibin.Li@nottingham.ac.uk)

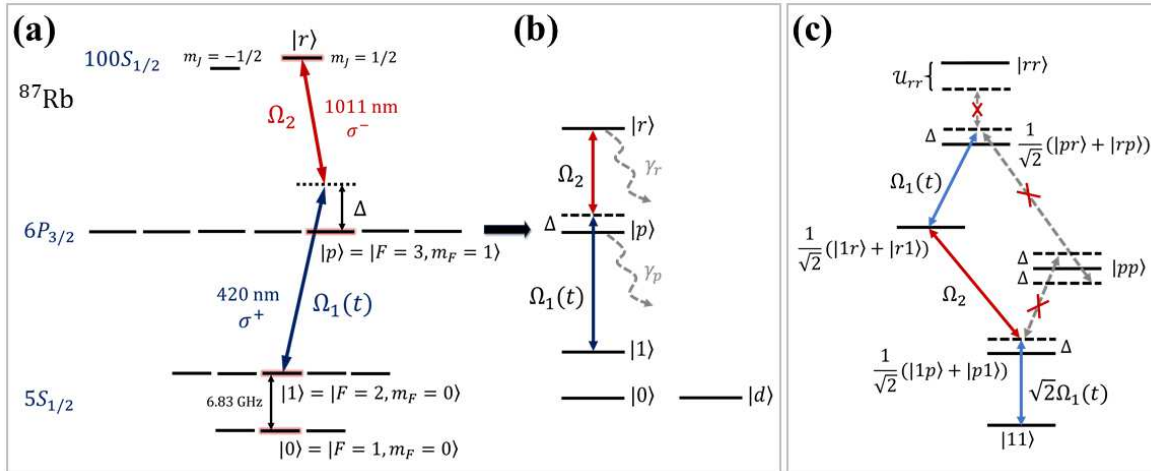


FIG. 1. (a) Relevant levels of <sup>87</sup>Rb. The  $5S_{1/2}$  hyperfine clock states  $|0\rangle \equiv |F = 1, m_F = 0\rangle$ ,  $|1\rangle \equiv |F = 2, m_F = 0\rangle$  are chosen as two ground states. To reach the Rydberg state we use two-photon excitation with wavelengths of 420 nm and 1011 nm. (b) Equivalent energy-level configuration of neutral atom qubit. Level  $|d\rangle$  is an uncoupled state representing the leakage levels outside qubit basis  $\{|0\rangle, |1\rangle\}$ . (c) The effective system dynamics initial from state  $|11\rangle$ , where  $U_{rr}$  is the vdW interaction between Rydberg states.

tensity variations compared with the standard protocol with constant-amplitude pulses.

Inspired by the work of Saffman *et al.* [80] and the protocols with single modulated driving pulse [61, 64], we here propose an improved adiabatic scheme to realize the standard  $C_z$  gate for Rydberg atoms. By symmetrically driving atoms with a single-modulated Gaussian pulse of blue detuned to the transition between ground state and the intermediate state, and a constant-amplitude pulse that red detuned to the transition between the intermediate state and the excited Rydberg state, we can acquire a dynamical phase factor of  $\pi$  accumulated on logic qubit state  $|11\rangle$  alone within the Rydberg blockade regime. The prominent advantages of our scheme are fourfold: (i) The Gaussian pulse takes the simple form of  $\Omega_0 \exp[-(t - 2T)^2/T^2]$ , and the corresponding optimal parameters can be easily determined by direct use of numerical integration. (ii) Considering spontaneous dissipation at room temperature, the gate fidelity of the system composed of <sup>87</sup>Rb atoms can reach 99.78% in less than 1  $\mu$ s, which is higher than the method with STIRAP pulses and catch up with the global optimal one [80]. (iii) Our scheme is beneficial to the realization of an arbitrary controlled-phase gate by only changing the width of the Gaussian pulse. (iv) Together with considering the technical imperfections in experiment, the predicted gate fidelity is able to maintain at about 98.4% for a realistic situation after correcting the detection errors, which may be helpful to the experimental implementation of quantum computation and quantum simulation in the neutral-atoms system.

The remainder of the paper is organized as follows. We first introduce the basic principle of the scheme and analytically show how the fast and high-fidelity  $C_z$  gate is adiabatically constructed in Sec. II. Then we discuss in detail the experimental feasibility and the gate errors introduced by technical imperfections, e.g. Doppler shifts and the fluctuation of Rydberg-Rydberg interaction strengths, the inhomogeneous Rabi frequency, the fluctuation and noise of external

fields, and the detection errors in Sec. III. Subsequently we briefly discuss the application of the proposed scheme to cesium atoms, and obtain that the gate fidelity can be achieved 99.81% by fully taking into account the spontaneous emission from intermediate and Rydberg states in Sec. IV. Finally, we make a conclusion in Sec. V.

## II. ADIABATICALLY CONTRIBUTION OF CONTROLLED-Z GATE

The controlled-Z ( $C_z$ ) gate is a two-qubit gate belonging to controlled unitary operations, which can accumulate a  $\pi$  phase on the target state  $|1\rangle$  if and only if the control qubit is in state  $|1\rangle$  [84, 85]. In the computational basis  $\{|00\rangle, |01\rangle, |10\rangle, |11\rangle\}$ , it can be defined as the unitary transformation

$$U_{Cz} = \begin{bmatrix} 1 & 0 & 0 & 0 \\ 0 & 1 & 0 & 0 \\ 0 & 0 & 1 & 0 \\ 0 & 0 & 0 & -1 \end{bmatrix}. \quad (1)$$

The physical system considered to realize this operation is a pair of <sup>87</sup>Rb atoms trapped in two tweezers with separation  $r$  shorter than the blocking radius, and the relevant levels are shown in Fig. 1(a). The logic qubit is encoded on  $|0\rangle \equiv |F = 1, m_F = 0\rangle$  and  $|1\rangle \equiv |F = 2, m_F = 0\rangle$  of  $5S_{1/2}$  hyperfine clock states with splitting  $2\pi \times 6.83$  GHz, and the Rydberg state  $|r\rangle \equiv |100S_{1/2}, m_j = 1/2\rangle$  is used to mediate the interaction between atoms. To coherently drive atoms from ground states to the Rydberg states, we apply two-photon excitation lasers, a  $\sigma^+$  polarized 420 nm laser and a  $\sigma^-$  polarized 1011 nm laser via the second resonance line  $|p\rangle \equiv |6P_{3/2}, F = 3, m_F = 1\rangle$  [56, 63] which possesses a longer lifetime and mitigates the power requirements for the same Rabi frequency compared with the first resonance line

in  $5P$  state. The simplified configuration of the atomic level is shown in Fig. 1(b), where we have introduced an uncoupled state  $|d\rangle$  denoting the leakage level outside  $|0\rangle$  and  $|1\rangle$  for simplicity. Thus, the master equation of the system in Lindblad form reads

$$\frac{d\rho}{dt} = -i[H_I, \rho] + \mathcal{L}_p[\rho] + \mathcal{L}_r[\rho], \quad (2)$$

where

$$H_I = \sum_{i=c,t} \frac{\Omega_1(t)}{2} |p\rangle_i \langle 1| + \frac{\Omega_2}{2} |r\rangle_i \langle p| + \text{H.c.} - \Delta |p\rangle_i \langle p| + \mathcal{U}_{rr} |rr\rangle \langle rr|, \quad (3)$$

describes the coherent dynamics of the system, and

$$\mathcal{L}_p[\rho] = \sum_{n=c,t} \sum_{i=0,1,d} L_{ip}^{(n)} \rho L_{ip}^{(n)\dagger} - \frac{1}{2} \{ L_{ip}^{(n)\dagger} L_{ip}^{(n)}, \rho \}, \quad (4)$$

$$\mathcal{L}_r[\rho] = \sum_{n=c,t} \sum_{j=0,1,d,p} L_{jr}^{(n)} \rho L_{jr}^{(n)\dagger} - \frac{1}{2} \{ L_{jr}^{(n)\dagger} L_{jr}^{(n)}, \rho \}, \quad (5)$$

describe spontaneous emission from  $|p\rangle$  and  $|r\rangle$  respectively with jump operator  $L_{jr(ip)}^{(n)} = \sqrt{b_{jr(ip)} \gamma_{r(p)}} |j(i)\rangle_n \langle r(p)|$  and  $b_{jr(ip)}$  denotes the branching ratio to the lower level  $|j(i)\rangle$ . At room temperature (300 K), the lifetime of state  $|p\rangle$  and  $|r\rangle$  are  $\tau_p = 0.118 \mu\text{s}$  and  $\tau_r = 353 \mu\text{s}$ , while the branching ratios are  $b_{0(1)p} = 1/8$ ,  $b_{dp} = 3/4$ ,  $d_{1(0)r} = 1/16$ ,  $d_{dr} = 3/8$ , and  $d_{pr} = 1/2$ . The term  $\mathcal{U}_{rr}$  characterizes the vdW interaction of  $-C_6/r^6$ , and the second-order non-degenerate perturbation theory gives that the dispersion coefficient  $C_6$  is about  $-56.171 \text{ THz}\cdot\mu\text{m}^6$  for Rydberg state  $|100S_{1/2}\rangle$  [86]. The reason why we choose  $ns$  state instead of  $nd$  state is that the interaction strength of  $ns$  is relatively isotropic, which is particularly important to keep our system still within the Rydberg blockade regime when considering the random thermal motion of atoms.

Now we discuss in detail the dynamic evolution of the four input states for the truth table of a standard two-qubit  $C_z$  gates, respectively. Since the ground state  $|0\rangle$  is decoupled to the external driving fields, the input state  $|00\rangle$  is stable during the gate operation, and the evolution form of the input states  $|01\rangle$  and  $|10\rangle$  are essentially the same as that of a single atom  $|1\rangle$ . Thus in the following we only consider the asymmetric state  $|01\rangle$  for the sake of convenience, and the Hamiltonian associated with it reads

$$H_{\text{eff}}^{(01)} = \frac{\Omega_1(t)}{2} |0p\rangle \langle 01| + \frac{\Omega_2}{2} |0r\rangle \langle 0p| + \text{H.c.} - \Delta |0p\rangle \langle 0p|, \quad (6)$$

which has a dark instantaneous eigenstate  $|\varphi(t)\rangle = \cos\vartheta |01\rangle - \sin\vartheta |0r\rangle$  with the mixing angle  $\vartheta = \arctan[-\Omega_1(t)/\Omega_2]$ . By properly modulating the shape of  $\Omega_1(t)$  with time so that the amplitude of its initial time and final time are close to zero and satisfying the adiabatic approximation condition simultaneously,

$$\left| \frac{2\Omega_2(\dot{\Omega}_1(t) - \Omega_1(t))}{\Delta + \sqrt{\Delta^2 + \Omega_1(t)^2 + \Omega_2^2}} \right| \ll 1, \quad (7)$$

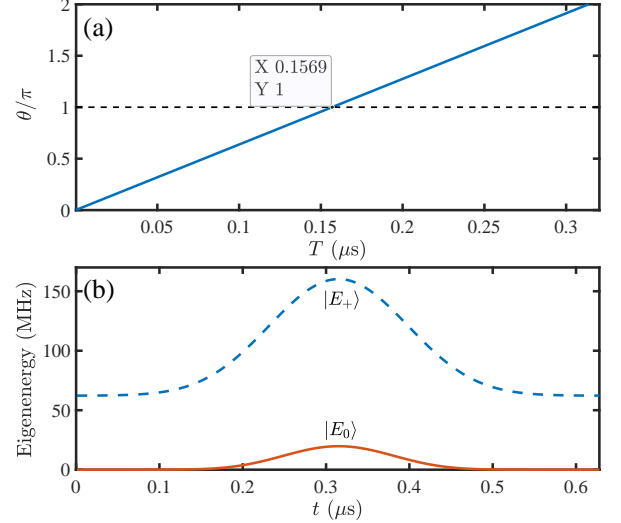


FIG. 2. (a) The relation between  $\theta = \int_0^{4T} E_0(t)dt$  and  $T$  under the parameters  $\Omega_0/2\pi = 160 \text{ MHz}$ ,  $\Omega_2/2\pi = 200 \text{ MHz}$  and  $\Delta/2\pi = 1000 \text{ MHz}$ , where  $\int_0^{4T} E_0(t)dt = \pi$  at  $T \approx 0.157 \mu\text{s}$ . (b) The eigenenergy  $|E_0\rangle$  and  $|E_+\rangle$  of the subsystem  $\{|11\rangle, |A\rangle, |B\rangle\}$  under the same parameters with  $T = 0.157 \mu\text{s}$ .

we can perform the cyclic evolution of state  $|01\rangle$  without accumulate any geometric phase or dynamic phase.

For the case where the input state is  $|11\rangle$ , the analysis is somewhat complicated. In Fig. 1(c), we give the transition path of relevant six symmetric states, where the population of state  $|rr\rangle$  is suppressed due to the Rydberg blockade and the states  $(|pr\rangle + |rp\rangle)/\sqrt{2}$  and  $|pp\rangle$  are less populated for large detuning  $2\Delta \gg \{\Omega_1(t)/2, \Omega_2/2\}$ . Therefore, we can safely neglect these processes and the effective Hamiltonian can be written as

$$H_{\text{eff}}^{(11)} = \frac{\sqrt{2}\Omega_1(t)}{2} |11\rangle \langle A| + \frac{\Omega_2}{2} |A\rangle \langle B| + \text{H.c.} - \Delta |A\rangle \langle A| + \frac{\Omega_1(t)^2}{4\Delta} |B\rangle \langle B|, \quad (8)$$

where  $|A\rangle = (|1p\rangle + |p1\rangle)/\sqrt{2}$  and  $|B\rangle = (|1r\rangle + |r1\rangle)/\sqrt{2}$ . Compared with the coherent trapping type Hamiltonian of Eq. (6), there is a shift  $\Omega_1(t)^2/4\Delta$  of the lower state  $|B\rangle$ . Although this energy shift is very small within the parameter range we set, its existence will significantly modify the dynamics of the system, making the evolution completely different from the traditional coherent trapping dynamics. The eigenvalues of  $H_{\text{eff}}^{(11)}$  are the roots of the secular equation which appears as a cubic characteristic equation

$$E^3 + aE^2 + bE + c = 0 \quad (9)$$

with  $a = \Delta - \Omega_1(t)^2/4\Delta$ ,  $b = -(3\Omega_1(t)^2 + \Omega_2^2)/4$  and  $c = \Omega_1^4/8\Delta$ . The solutions to this cubic equation are

$$E_0(t) = \frac{2}{3} \left( -\frac{\Delta}{2} + \frac{\Omega_1(t)^2}{8\Delta} + \tilde{\Omega} \cos\left[\frac{\zeta}{3}\right] \right), \quad (10)$$

$$E_{\pm}(t) = \frac{2}{3} \left( -\frac{\Delta}{2} + \frac{\Omega_1(t)^2}{8\Delta} + \tilde{\Omega} \cos\left[\frac{2\pi \mp \zeta}{3}\right] \right), \quad (11)$$

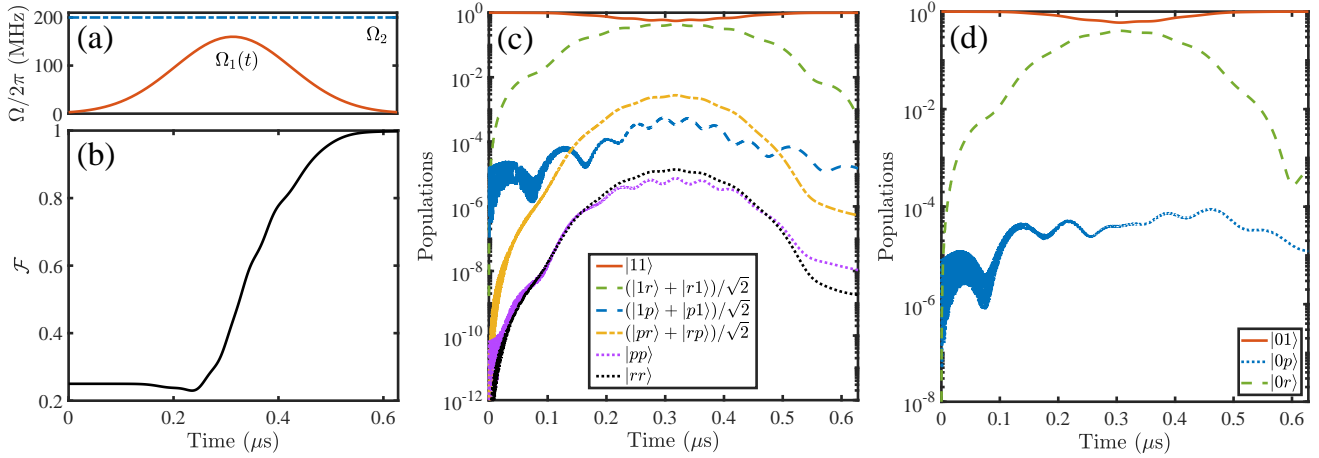


FIG. 3. The realization of the  $C_z$  gate governed by the master equation (2). (a) The time dependence of Rabi frequency of application. (b) The fidelity of the  $C_z$  gate. (c) Populations of states  $|11\rangle$ ,  $|pp\rangle$ ,  $(|1r\rangle + |r1\rangle)/\sqrt{2}$ ,  $(|1p\rangle + |p1\rangle)/\sqrt{2}$ ,  $(|pr\rangle + |rp\rangle)/\sqrt{2}$ ,  $|rr\rangle$  for the initial state  $|11\rangle$ . (d) Populations of the  $|01\rangle$ ,  $|0p\rangle$  and  $|0r\rangle$  states for initial state  $|01\rangle$ . The parameters are taken as  $\Omega_0/2\pi = 160$  MHz,  $\Omega_2/2\pi = 200$  MHz,  $\Delta/2\pi = 1000$  MHz,  $\mathcal{U}_{rr}/2\pi = 2$  GHz,  $T = 0.157\ \mu\text{s}$ ,  $\tau_r = 353\ \mu\text{s}$  and  $\tau_p = 0.118\ \mu\text{s}$ .

with

$$\tilde{\Omega} = \frac{1}{2} [7\Omega_1(t)^2 + 3\Omega_2^2 + 4\Delta^2 + \frac{\Omega_1(t)^4}{4\Delta^2}]^{1/2}, \quad (12)$$

$$\zeta = 2\pi - \arccos\{-[64\Delta^6 - \Omega_1(t)^6 + 24\Delta^4(7\Omega_1(t)^2 + 3\Omega_2^2) + 6\Delta^2(11\Omega_1(t)^4 - 3\Omega_2^2\Omega_1(t)^2)]/64\Delta^3\tilde{\Omega}^3\} \quad (13)$$

The corresponding eigenvectors can be constructed as

$$|E_0(t)\rangle = \cos\Theta|11\rangle + \sin\Phi\sin\Theta|A\rangle - \cos\Phi\sin\Theta|B\rangle, \quad (14)$$

$$|E_+(t)\rangle = (\cos\Phi\cos\Theta\sin\phi + \sin\Phi\cos\phi)|B\rangle - (\sin\Phi\cos\Theta\sin\phi - \cos\Phi\cos\phi)|A\rangle + \sin\Theta\sin\phi|11\rangle,$$

$$|E_-(t)\rangle = (\cos\Phi\cos\Theta\cos\phi - \sin\Phi\sin\phi)|B\rangle - (\sin\Phi\cos\Theta\cos\phi + \cos\Phi\sin\phi)|A\rangle + \sin\Theta\cos\phi|11\rangle,$$

where

$$\Theta = \arctan\{\frac{\Omega_1(t)[(E_0(t) - \Omega_1(t)^2/4\Delta)^2 + \Omega_2^2/4]^{1/2}}{\sqrt{2}[(E_0(t) + \Delta)(E_0(t) - \Omega_1(t)^2/4\Delta) - \Omega_2^2/4]}\}, \quad (15)$$

$$\Phi = \arctan\{-\frac{2E_0(t) - \Omega_1(t)^2/2\Delta}{\Omega_2}\}, \quad (16)$$

and it is not possible to find one expression for  $\phi$  that is valid for all values of the parameters [87, 88]. Fortunately, this uncertainty does not affect our numerical simulation results below. At  $t = 0$ ,  $E_0(0) \rightarrow 0$  and  $|E_0(0)\rangle \approx \cos\Theta|11\rangle - \sin\Theta|B\rangle \approx |11\rangle$  because of  $\Theta \approx \arctan[-\sqrt{2}\Omega_1(0)/\Omega_2] \approx 0$ . Therefore under the adiabatic evolution condition of this case

$$\left| \frac{\langle E_0(t)|\dot{E}_\pm(t)\rangle}{E_\pm(t) - E_0(t)} \right| \ll 1, \quad (17)$$

the state  $|11\rangle$  evolves along the eigenstate  $|E_0(t)\rangle$  from beginning to end as

$$|\Psi(t)\rangle = e^{-i\int_0^t E_0(t')dt'}|E_0(t)\rangle, \quad (18)$$

from which a dynamical phase  $-\int_0^{T_g} E_0(t')dt'$  is acquired after state  $|11\rangle$  undergoing a cyclic evolution over the gate operation time  $T_g$ .

Remarkably, there are many options for time-dependent modulation pulses that meet the condition of our scheme. For the convenience of experimental implementation, we here consider the time-dependent Rabi frequency  $\Omega_1(t)$  as a Gaussian pulse which takes the form of

$$\Omega_1(t) = \Omega_0 e^{-\frac{(t-2T)^2}{T^2}}, \quad (19)$$

where  $\Omega_0$  and  $T$  are the maximum amplitude and width of the Gaussian pulse, respectively. On the basis of which, the evolution time of the system should be set as  $T_g = 4T$  since the pulse  $\Omega_1(t)$  peaks at  $t = 2T$ . In order to realize the two-

TABLE I. The relationship among the fidelity of the  $C_z$  gate, the evolution time  $4T$ , and  $\Omega_0$ . The other parameters are taken as  $\Omega_2/2\pi = 200$  MHz,  $\Delta/2\pi = 1000$  MHz,  $\mathcal{U}_{rr}/2\pi = 2$  GHz.

$\Omega_0/2\pi$ (MHz)	100	120	140	160	180
$4T$ ( $\mu$ s)	2.7956	1.5352	0.9428	0.628	0.444
$\mathcal{F}_t(\gamma = 0)$	0.9999	0.9997	0.9993	0.9990	0.9976
$\mathcal{F}_t(\gamma \neq 0)$	0.9984	0.9984	0.9980	0.9978	0.9963

qubit  $C_z$  gate, we need

$$\int_0^{4T} E_0(t') dt' = \pm\pi. \quad (20)$$

From the above analyses, we know that only  $|11\rangle$  will accumulate an effective dynamic phase through the non-zero eigenenergy. Thus, to determine the adjustable evolution time  $4T$ , we have to solve the function Eq. (20). However, due to the complicated form of  $E_0(t)$ , the analytic form of the integral is difficult to calculate. We scan the numerical integration results with different  $T$  instead and try to find the point where the integral is  $\pi$ . Starting from initial state  $|\Psi(0)\rangle = (|00\rangle + |01\rangle + |10\rangle + |11\rangle)/2$ , the fidelity  $\mathcal{F}$  of the  $C_z$  gate is defined by the population of the target state  $|\Psi_t\rangle = (|00\rangle + |01\rangle + |10\rangle - |11\rangle)/2$ . It should be noted that the definition of gate fidelity used here is essentially the same as the definition of Bell-state fidelity used in the previous literature [60, 80]. To achieve the Rydberg strong blockade, we choose  $\mathcal{U}_{rr}/2\pi = 2$  GHz which corresponds to a interatomic spacing  $r \simeq 5.5$   $\mu$ m. Moreover, by fixing the parameters  $\Omega_2/2\pi = 200$  MHz and  $\Delta/2\pi = 1000$  MHz, the relationship among the fidelity of the  $C_z$  gate, the evolution time  $4T$ , and the parameter  $\Omega_0$  is shown in Table. I which is governed by Eq. (2). Theoretically speaking, for a smaller  $\Omega_0$ ,  $\mathcal{F}_t$  can reach over 0.9999 without considering the spontaneous emissions. However, this condition results in a long evolution time which may deepen the influences of spontaneous emissions and dephasing. For the above reasons, we select  $\Omega_0/2\pi = 160$  MHz in the following analysis to implement a relatively fast and high-fidelity logic gate.

According to the relevant levels of  $^{87}\text{Rb}$ , the  $|1\rangle \rightarrow |p\rangle$  transition is driven by a 420 nm beam with typical beam power  $P_0 = 78.5$   $\mu$ W and waist of  $\omega_{x|y,0} = 4.2$   $\mu$ m which gives a Rabi frequency  $\Omega_0/2\pi = 160$  MHz. By tuning the 1011 nm beam with typical beam power  $P_2 = 290.5$  mW and waist of  $\omega_{x|y,2} = 3.9$   $\mu$ m, the transition of  $|p\rangle \rightarrow |r\rangle$  can be realized with Rabi frequency  $\Omega_2/2\pi = 200$  MHz. In addition, these two beams are tuned about  $\Delta/2\pi = 1$  GHz to the blue (red) of the  $|1\rangle \rightarrow |p\rangle$  ( $|p\rangle \rightarrow |r\rangle$ ) transition. As shown in Fig. 2(a), after scanning the numerical integration results, we have  $T = 0.157$   $\mu$ s under such parameters. Fig. 2(b) illustrates the eigenenergy spectrum of the system in the subspace  $\{|11\rangle, |A\rangle, |B\rangle\}$  varying with time. The large gap between  $E_0(t)$  and  $E_+(t)$  promises a nearly perfect coherent population transfer process. This feature brings another advantage of our scheme over the previous methods [60, 73], which is beneficial to the realization of an arbitrary controlled-phase

gate

$$U_{Cz} = \begin{bmatrix} 1 & 0 & 0 & 0 \\ 0 & 1 & 0 & 0 \\ 0 & 0 & 1 & 0 \\ 0 & 0 & 0 & e^{i\theta} \end{bmatrix}. \quad (21)$$

Fig. 2(a) also shows how an arbitrary phase  $\theta$  can be acquired from 0 to  $2\pi$  by changing the shape of Gaussian pulse via the parameter  $T$  alone. Fig. 3 depicts the dynamics of each input state and Rabi frequency with time under given parameters  $\Omega_0/2\pi = 160$  MHz,  $\Omega_2/2\pi = 200$  MHz,  $\Delta/2\pi = 1000$  MHz,  $\mathcal{U}_{rr}/2\pi = 2$  GHz,  $T = 0.157$   $\mu$ s,  $\tau_r = 353$   $\mu$ s and  $\tau_p = 0.118$   $\mu$ s, which is confirmed again that the symmetric states  $|rr\rangle$ ,  $(|pr\rangle + |rp\rangle)/\sqrt{2}$ , and  $|pp\rangle$  are well suppressed during the process of realizing  $C_z$  gate.

### III. DISCUSSION OF THE EXPERIMENTAL FEASIBILITY AND TECHNICAL IMPERFECTIONS

Because the atomic thermal motion and the large spontaneous emission rate at room temperature will harm our scheme, we need to cool the atom to a lower temperature. Experimentally, Magneto-optical trap (MOT) technology based on the Doppler cooling mechanism is the most commonly used laser cooling and trapping method, which provides a platform for many scientific research and applications using cold atomic systems [89, 90]. However, since MOT cannot store the quantum state for a long time, it is necessary to add additional capture methods without affecting the control of quantum states. Another more important reason is that the atomic cooling and trapping scales of MOT vary from several hundred microns to several millimeters much larger than the Rydberg blocking radius. Therefore, in the experiment, the neutral atom is loaded into a far resonance optical trap (FORT) [52, 56] or an optical tweezer [91–93] via MOT to achieve further capture. The optical dipole trap is based on the so-called dipole force. A tightly focused laser beam can trap atoms in its focal center and form so-called optical tweezers or optical dipole traps. The trapping potential of a far-off-resonant optical tweezer with linearly polarized light can be described by [94, 95]

$$U_F(\mathbf{r}) = \frac{\pi c^2 \Gamma}{2\omega_0^3} \left( \frac{2}{\Delta_{3/2}} + \frac{1}{\Delta_{1/2}} \right) I(\mathbf{r}), \quad (22)$$

where  $\omega_0$  and  $\Gamma$  are the frequency and decay rate of  $5S_{1/2} - 5P_{3/2}$  transition and  $\Delta_{3/2(1/2)}$  is the laser detuning from the  $5P_{3/2(1/2)}$ . The trap depth can be obtained combined with the presence of peak trapping intensity  $I(0) = 2P_f/\pi\omega_f^2$ . The experimental apparatus used in the recent  $C_z$  gate scheme proposed by Fu *et al.* can cool the atomic temperature to 5.2  $\mu$ K in a 50  $\mu$ K trap by applying polarization-gradient cooling and adiabatic [64]. A similar experimental device can be applied to our scheme. The possible experimental structure is shown in Fig. 4, where two  $^{87}\text{Rb}$  atoms are individually trapped in two separated optical tweezers generated by the tightly focused laser beams with wavelength  $\lambda_f = 830$  nm propagating

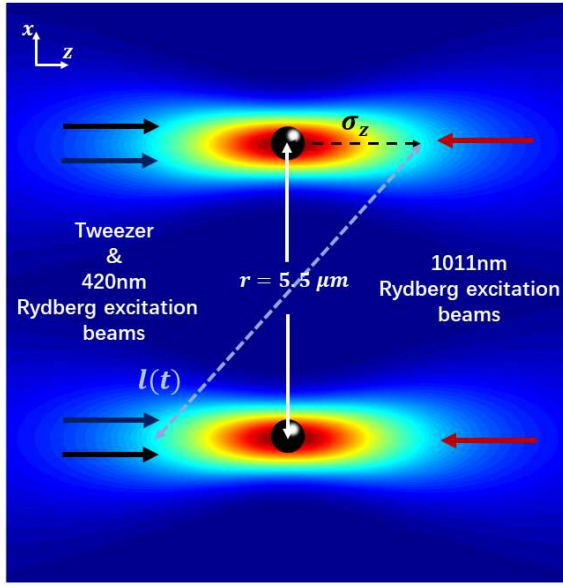


FIG. 4. Experimental geometry. Two single atoms are trapped in two tweezers separated by about  $5.5 \mu\text{m}$  with tweezer beam and Rydberg excitation beams propagating along quantized  $z$ -axis.

along the quantized  $z$ -axis and separated by  $5.5 \mu\text{m}$ . The typical beam power of which is  $P_f = 174 \mu\text{W}$  to a waist ( $1/e^2$  intensity radius) of  $\omega_f = 1.2 \mu\text{m}$ .

As studied in Ref. [96], we respectively numerically analyze the technical imperfections in four aspects : (i) Doppler shift and the fluctuation of Rydberg-Rydberg interaction strengths, (ii) the inhomogeneous Rabi frequency, (iii) fluctuation and noise of external fields, and (vi) finite detection errors. The detailed analyses are listed below in subsections. To be more credible, in later simulations we show the results average over a hundred realizations by considering fluctuations of the above parameters.

### A. Doppler shifts and fluctuation of Rydberg-Rydberg interaction strength

Due to the limitation of the existing cooling mechanism, the temperature of the atom cannot reach absolute zero. Therefore, the atom has a certain speed which will lead to the Doppler effect, and the laser frequency detuning felt by the atom will be shifted from  $\Delta$ . In addition, atoms affected by non-zero temperature will cause vibrations near the ideal position. Synthesize these two reasons, the actual distance  $l(t)$  between the two atoms changes over time which introduces the fluctuation of Rydberg-Rydberg interaction strengths. The ideal position of the control and target atoms are denoted as  $\mathbf{R}_c = (0, 0, 0)$  and  $\mathbf{R}_t = (r, 0, 0)$ , respectively. The Hamiltonian includes the atomic motion and the fluctuation of vdW interaction is shown as [97]

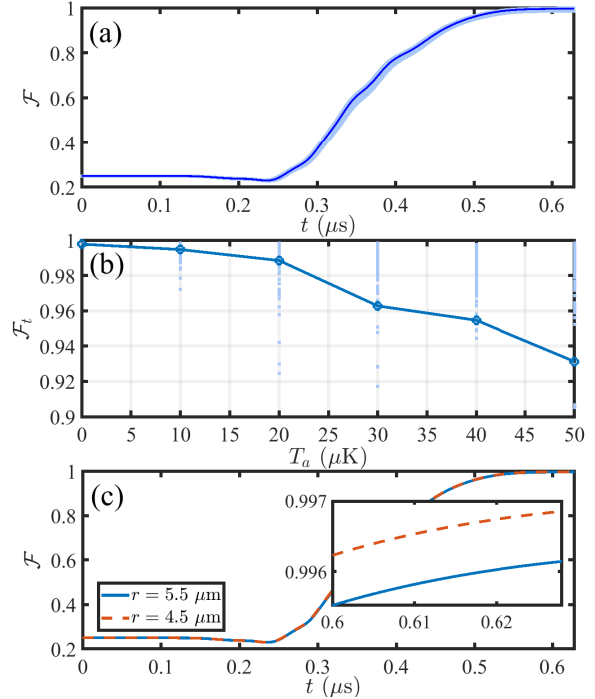


FIG. 5. (a) The system dynamics considering the Doppler effect and the fluctuation of vdW interaction at the finite temperature  $T_a = 5.2 \mu\text{K}$  governed by the master equation (2) with Hamiltonian (26). (b) The gate fidelity at different temperature  $T_a$ . (c) The average evolution results with initial separation  $r = 5.5 \mu\text{m}$  (solid line) and  $r = 4.5 \mu\text{m}$  (dashed line), respectively. Note that the light blue region show the results of a hundred stochastic simulations and the solid line in dark blue corresponds to the average results. The parameters are taken as same as Fig. 3.

$$H_v = \sum_{i=c,t} \frac{\Omega_1(t)}{2} e^{i\mathbf{k}_1 \cdot \mathbf{R}_i(t)} |p\rangle_i \langle 1| + \frac{\Omega_2}{2} e^{i\mathbf{k}_2 \cdot \mathbf{R}_i(t)} |r\rangle_i \langle p| + \text{H.c.} - \Delta |p\rangle_i \langle p| + \mathcal{U}_{rr}[l(t)] |rr\rangle \langle rr|, \quad (23)$$

where  $\mathbf{R}_i(\tau) = \mathbf{R}_i + \delta\mathbf{R}_i + \mathbf{v}_i t$  and  $l(t) = |\mathbf{R}_c(t) - \mathbf{R}_t(t)|$  as shown in Fig. 4. The randomly generated three-dimensional position  $\delta\mathbf{R}_i$  and velocity vector  $\mathbf{v}_i$  obey the Maxwell-Boltzmann distribution. The time-averaged variances of atomic position and momentum are shown as [52]

$$\langle x^2 \rangle = \langle y^2 \rangle = \frac{\omega_f^2}{4} \frac{T_a}{|U_F|}, \quad \langle z^2 \rangle = \frac{\pi^2 \omega_f^4}{2 \lambda_f^2} \frac{T_a}{|U_F|}, \quad (24)$$

$$\langle v_x^2 \rangle = \langle v_y^2 \rangle = \langle v_z^2 \rangle = \frac{T_a}{m}, \quad (25)$$

where  $T_a$  is the measured temperature of the trapped atoms. In our setup [Fig. 4], the two excitation lasers with vectors  $\mathbf{k}_1$  and  $\mathbf{k}_2$  are counter-propagating along  $z$ -axis. The Hamiltonian can be rewritten as

$$H_v = \sum_{i=c,t} \frac{\Omega_1(t)}{2} e^{i\mathbf{k}_1^z Z_i(t)} |p\rangle_i \langle 1| + \frac{\Omega_2}{2} e^{-i\mathbf{k}_2^z Z_i(t)} |r\rangle_i \langle p| + \text{H.c.} - \Delta |p\rangle_i \langle p| + \mathcal{U}_{rr}[l(t)] |rr\rangle \langle rr|, \quad (26)$$

where  $Z_i = z_i + \delta z_i + v_{zi}t$ . The corresponding wave vectors are  $k_{z1}/2\pi \simeq 2.381 \times 10^6 \text{ /m}$  and  $k_{z2}/2\pi \simeq 0.988 \times 10^6 \text{ /m}$ . The vdW interaction at every moment is  $\mathcal{U}_{rr}[l(t)]/2\pi = -C_6/l(t)^6$ . Assuming the position distribution and velocity vector of two atoms are both Gaussian with variance of

$$\sigma_x^2 = k_B \langle x^2 \rangle, \quad \sigma_y^2 = k_B \langle y^2 \rangle, \quad \sigma_z^2 = k_B \langle z^2 \rangle, \quad (27)$$

$$\sigma_{v_x}^2 = k_B \langle v_x^2 \rangle, \quad \sigma_{v_y}^2 = k_B \langle v_y^2 \rangle, \quad \sigma_{v_z}^2 = k_B \langle v_z^2 \rangle, \quad (28)$$

where  $k_B$  is the Boltzmann constant. The random numbers obeying such Gaussian distribution can be obtained with two uniformly distributed random numbers  $\xi$  in the interval  $[0, 1]$  denoted as  $\sigma_i \sqrt{-2 \ln \xi_1} \cos[2\pi \xi_2]$ .

Fig. 5(a) shows the fidelity of  $C_z$  gate governed by the master equation with Hamiltonian (26) under  $T_a = 5.2 \mu\text{K}$ . The light blue parts show the results of a hundred times stochastic simulations and the solid line in dark blue corresponds to the average result. The average gate error is about 0.00162. Fig. 5(b) shows the dependence of the gate fidelity on different atomic temperatures  $T_a$  which illustrates that the lower cooling temperature is beneficial to the generation of the gate. The reason is that  $\mathcal{U}_{rr}$  is dependent on the atomic separation  $l(t)$ . With the increase of  $T_a$ , the range of atomic motion expands, which cannot guarantee the strong Rydberg blockade and lead to a greater error. According to our setup, the gate fidelity can hold above 0.98 with  $T_a < 20 \mu\text{K}$ . Since the implementation of the Rydberg atomic blockade is related to the distance between atoms, Fig. 5(c) respectively plot the evolution results on average under  $r = 5.5 \mu\text{m}$  and  $r = 4.5 \mu\text{m}$  with  $T_a = 5.2 \mu\text{K}$  which illustrate that the error can be further reduced by narrowing the initial distance between atoms. In addition, under the influence of atomic temperature, atomic vibration is more intense in the direction of the tweezer beam. Therefore, we make the atoms arranged perpendicular to the direction of the tweezer beam to reduce the effect of atomic vibration.

## B. Inhomogeneous Rabi frequency

In the above section, we have discussed the influence of relative phase and fluctuation of vdW interaction caused by atomic vibration at finite temperature. But subject to the beam waists of lasers, the optical intensity of laser interacting with atoms changes with the vibration of atoms in beam alignment resulting in an extra gate error. The spatial dependence of Rabi frequency has been studied in Ref. [98]. The position-dependent Rabi frequencies can be written as [56]

$$\Omega_1(t, \tilde{\mathbf{R}}_i) = \Omega_1(t, 0) \frac{e^{-[\frac{x^2}{\omega_{x,0}^2(1+z^2/L_{x,0}^2)} + \frac{y^2}{\omega_{y,1}^2(1+z^2/L_{y,0}^2)}]}}{[(1+z^2/L_{x,0}^2)(1+z^2/L_{y,0}^2)]^{1/4}}, \quad (29)$$

$$\Omega_2(\tilde{\mathbf{R}}_i) = \Omega_2(0) \frac{e^{-[\frac{x^2}{\omega_{x,2}^2(1+z^2/L_{x,2}^2)} + \frac{y^2}{\omega_{y,2}^2(1+z^2/L_{y,2}^2)}]}}{[(1+z^2/L_{x,2}^2)(1+z^2/L_{y,2}^2)]^{1/4}}, \quad (30)$$

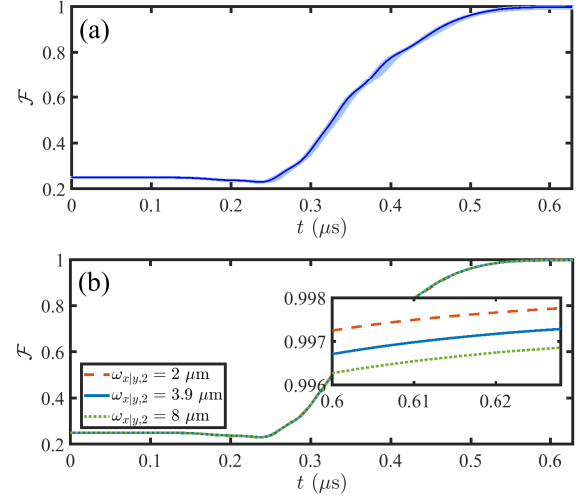


FIG. 6. (a) The system dynamics considering the inhomogeneous Rabi frequency governed by the master equation (2) with position-dependent Rabi frequencies  $\Omega_1(t, \tilde{\mathbf{R}}_i)$  and  $\Omega_2(\tilde{\mathbf{R}}_i)$  (b) The average results under different beam waists of  $\Omega_2$ .

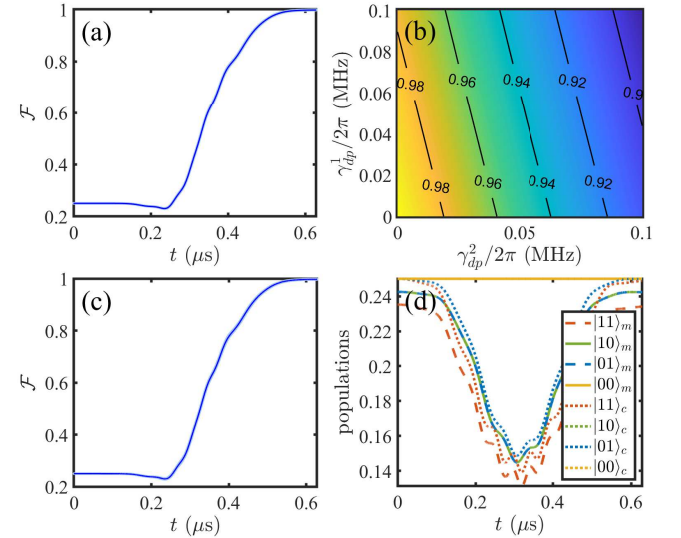


FIG. 7. (a) The system dynamics considering the fluctuation of the Rabi frequency governed by the master equation (2) with Hamiltonian (31). (b) The gate fidelities with laser phase noise governed by Eq. (2) plus (32). (c) The system dynamics with detuning  $\delta \neq 0$ . (d) The measured and corrected populations of states  $|11\rangle$ ,  $|10\rangle$ ,  $|01\rangle$  and  $|00\rangle$  with initial state  $|\Psi(0)\rangle = 1/2(|00\rangle + |01\rangle + |10\rangle + |11\rangle)$  and finite detection errors  $(\epsilon, \epsilon') = (0.03, 0.0047)$ .

where  $\Omega_1(t, 0)$  and  $\Omega_2(0)$  are the Rabi frequencies at trap center,  $L_{x|y,i} = \pi \omega_{x|y,i}^2 / \lambda_i$  is the Rayleigh length. The trap position of atom  $i$  is  $\tilde{\mathbf{R}}_i = \tilde{\mathbf{R}}_i + \delta \mathbf{R}_i$ , where  $\tilde{\mathbf{R}}_i$  is the ideal position denotes the laser alignment. Because two atoms are driven independently, the definition of  $\tilde{\mathbf{R}}_i$  equals  $(0, 0, 0)$  independent of the relative position of atoms. Fig. 6(a) shows the gate fidelity with the atom temperature  $T_a = 5.2 \mu\text{K}$

where the inhomogeneous Rabi frequency has a little influence and the average fidelity can reach about 0.9973. In addition, the waist of the drive pulses influences the gate fidelity under the same atomic temperature. As shown in Fig. 6(b), we plot the average evolution results with different beam waists of  $\Omega_2$ . It illustrates that the wider beam waist is more conducive to the realization of the gate.

### C. Fluctuation and noise of external fields

During the experiment, multiple fields are applied, such as the laser fields used to drive atoms and the magnetic fields used to lift the degeneracy of the Zeeman sublevels. The gate errors introduced by the fluctuation and noise of these external fields will be discussed in this section.

(i) The fluctuation of the Rabi frequency. The intensity fluctuation of laser fields will introduce a fluctuation  $\delta I_i$  on the driving Rabi frequency which is assumed to follow the normal distribution functions with the standard deviations  $\sigma_{I_i} \approx 0.05\Omega_i$ . The system Hamiltonian is shown as

$$H_\Omega = \sum_{i=c,t} \frac{1}{2}[\Omega_1(t) + \delta I_1] |p\rangle_i \langle 1| + \frac{1}{2}(\Omega_2 + \delta I_2) |r\rangle_i \langle p| + \text{H.c.} - \Delta |p\rangle_i \langle p| + \mathcal{U}_{rr} |rr\rangle \langle rr|. \quad (31)$$

As shown in Fig. 7(a) the average result can still reach  $\mathcal{F} = 0.9978$  after a hundred times experiment, which has little influence on our method.

(ii) The phase noise of laser fields. The laser phase noise can be directly written as  $\Omega_i(t) = \Omega_i \exp(i\varphi_i(t))$ , where  $\varphi_i(t)$  presents as a random process related to the power spectral density  $S_\varphi(f)$  with phase-modulated Fourier frequency  $f$ . Because  $S_\varphi(f)$  depends on the test results of specific experiments, the laser phase noise is difficult to quantify directly [99, 100]. But the average result of the laser phase noise will lead to dephasing of Rabi oscillations [96]. The system appears dephasing behaviour which can be described as

$$\mathcal{L}_{li}[\rho] = \sum_{n=1}^2 L_{li}^{(n)} \rho L_{li}^{(n)\dagger} - \frac{1}{2} \{ L_{li}^{(n)\dagger} L_{li}^{(n)}, \rho \}, \quad (32)$$

In which, the Lindblad operators are shown as  $\mathcal{L}_{l1} = \sqrt{\gamma_{dp}^1}/2 (|p\rangle \langle p| - |1\rangle \langle 1|)$  and  $\mathcal{L}_{l2} = \sqrt{\gamma_{dp}^2}/2 (|r\rangle \langle r| - |p\rangle \langle p|)$  describing the dephasing between  $|p\rangle$  and  $|1\rangle$  and between  $|r\rangle$  and  $|p\rangle$  caused by the phase noise of  $\Omega_1(t)$  and  $\Omega_2$ , respectively. Fig. 7(b) shows the gate fidelity governed by the master equation (2) plus (32) with  $\gamma_{dp}^{1(2)}/2\pi \in [0, 0.1]$  MHz.

(iii) The fluctuation of the detuning. The fluctuations of the external magnetic field cause transition shift, giving a Rydberg two-photon detuning  $\Delta_B = (g_r m_r - g_1 m_1) \mu_B B_z$ , where  $g_r = 2$  and  $g_1 = 1/2$  are Landé factors, while  $m_r = 1/2$  and  $m_1 = 0$ . The fluctuations of the excitation laser frequencies and the light shift will also destroy the two-photon resonance process and introduce another detuning  $\Delta_l$ .

The system Hamiltonian is shown as

$$H_I = \sum_{i=c,t} \frac{\Omega_1(t)}{2} |p\rangle_i \langle 1| + \frac{\Omega_2}{2} |r\rangle_i \langle p| + \text{H.c.} - \Delta |p\rangle_i \langle p| - \frac{\delta}{2} (|1\rangle_i \langle 1| - |r\rangle_i \langle r|) + \mathcal{U}_{rr} |rr\rangle \langle rr|, \quad (33)$$

where detuning  $\delta = \Delta_B + \Delta_l$  unequal to zero takes into account the above fluctuations. Combined with a variety of experiments, we consider the fluctuation of the detuning follows the normal distribution with the standard deviation  $\sigma_\delta$  on the order of several hundred kHz for simplicity. To give the results more credibility, we choose a larger standard deviation  $\sigma_\delta/2\pi = 500$  kHz here. As Fig. 7(c) shows, this fluctuation takes little effect.

### D. Detection errors

According to Ref. [96], the detection errors can be divided into two parts: (i) the “false positive” errors and (ii) the “false negative” errors. For the “false positive” errors, it refers to the incorrect infer of the ground-state atom was in  $|r\rangle$  which can be denoted as  $\epsilon = P(r|1)$ . This contains the motion loss of atoms when we turn off the optical traps during the  $C_z$  gate or due to the background-gas collisions. The measured value of  $\epsilon$  is typical  $0.01 - 0.03$ . For the “false negative” errors, it can be denoted as  $\epsilon' = P(1|r)$  which is introduced by the spontaneous emission from  $|r\rangle$  to  $|1\rangle$  before the atom escaping. These errors can approximate by  $\epsilon' = \gamma_r t_{\text{recap}}/n$  for  $n > 50$ , where  $t_{\text{recap}} = 1/\gamma_{pi}$  [52, 99].  $\gamma_{pi}$  is the ionization rate of the Rydberg atom which is proportional to  $U_F$  and inversely proportional to  $n^3$  where  $n$  is the principal quantum number. In Ref. [52], it shows that the ionization rate  $\gamma_{pi}$  of the Rydberg atom with  $n = 50$  and  $U_F = 1$  mK is about 31000/s. As a rough approximation, we can estimate the ionization rate corresponding to other principal quantum numbers by scaling this value like

$$\gamma_{pi} = \frac{U_F}{1\text{mK}} \left( \frac{n}{50} \right)^{-3} (31000)/\text{s}. \quad (34)$$

And then the finite error  $\epsilon'$  can be estimated as  $\epsilon' \approx 0.0047$  including the effective lifetime of Rydberg state  $100S_{1/2}$  and the measured atomic temperature. To numerically measure the gate fidelity, the state measured at the final time can be denoted as  $|\psi_t\rangle_m = \alpha|00\rangle + \beta|01\rangle + \zeta|10\rangle + \eta e^{i\phi(t)}|11\rangle$ , where

$$|\eta|^2 = (1 - \epsilon)^2 \tilde{P}_{11} + (1 - \epsilon) \epsilon' \tilde{P}_{1r} + \epsilon' (1 - \epsilon) \tilde{P}_{r1} + \epsilon'^2 \tilde{P}_{rr}, \quad (35)$$

$$|\zeta|^2 = (1 - \epsilon) \tilde{P}_{10} + \epsilon' \tilde{P}_{r0}, \quad (36)$$

$$|\beta|^2 = (1 - \epsilon) \tilde{P}_{01} + \epsilon' \tilde{P}_{0r}. \quad (37)$$

$\tilde{P}_{jk}$  represents the population of state  $|jk\rangle$  numerically. After numerical simulations, we plot the actual and corrected populations of states  $|11\rangle$ ,  $|10\rangle$ ,  $|01\rangle$  and  $|00\rangle$ , respectively. The

TABLE II. Fidelity errors of the gate corresponding to the system constructed by  $^{87}\text{Rb}$  atoms trapped in two optical tweezers shown in Ref. [64]. The tweezers are generated by the tightly focused 830 nm laser, with beam waist at focal plane  $1.2(1) \mu\text{m}$  with trap depth  $50 \mu\text{K}$  and the temperature of single-atom is about  $T_a = 5.2 \mu\text{K}$ . The lower section gives the average results after a hundred times numerical simulation.

Quantity	Error	Fidelity estimate
Spontaneous emission	0.00124	
Doppler effects and the fluctuation of Rydberg-Rydberg interaction strengths	0.00162	
The inhomogeneous Rabi frequency	0.00048	
The fluctuation of Rabi frequency	-0.000016	
Laser noises ( $\gamma_{dp}/2\pi = 10 \text{ kHz}$ )	0.01151	
Fluctuation of detuning	-0.000006	$\mathcal{F}_{Cz} \simeq 0.9842$
Detection errors	0.01 $\sim$ 0.03	$\mathcal{F}_{Cz} \simeq 0.9742 \sim 0.9542$

initial state is taken as  $|\Psi(0)\rangle$ . As shown in Fig. 7(d), the dotted lines are corresponding to the measured results. With  $(\epsilon, \epsilon') = (0.03, 0.0047)$ , the detection error on fidelity is about 0.03 while with  $(\epsilon, \epsilon') = (0.01, 0.0047)$  the detection error on fidelity is about 0.01. However, these errors can be reduced by improve the detection method, such as applying strong electric field, increasing the measuring speed and improving vacuum conditions [58, 99].

In conclusion, Table. II summarizes the gate errors under different technical imperfections. Among them, dephasing caused by laser phase noise has the greatest influence. And the fluctuations of laser intensity and detuning have the smallest influence even increasing the fidelity a little because of the randomness. After correcting the detection errors, the predicted gate fidelity in the experiment can reach about 0.984 in our scheme. On the other respect, in our scheme, by widening the waists of Rydberg excitation beams, the atoms can also be globally driven because of the small separation required for the Rydberg blockade [64]. However, for the laser with a wider beam waist, the laser power should also be increased to achieve the required Rabi frequency. In contrast, by changing the direction of the external magnetic field so that the Rydberg excitation beams relatively propagate along the  $X$ -axis in Fig. 4, i.e. perpendicular to the trap direction, the global drive can be achieved without increasing the beam waists [101]. Since the relative positions of atoms vary in the same range as the independent drive method, the error caused by atomic motion, such as Doppler shifts and the inhomogenous Rabi frequency, will not change significantly.

#### IV. APPLICATION TO $^{133}\text{Cs}$

To make a comparison with previous schemes [77, 80], we further measure the fidelity of the  $C_z$  gate with  $^{133}\text{Cs}$  atoms. We choose the  $6S_{1/2}$  hyperfine clock states as ground states  $|0\rangle \equiv |F = 3, m_F = 0\rangle$ ,  $|1\rangle \equiv |F = 4, m_F = 0\rangle$  and the Rydberg state  $|r\rangle \equiv |126S_{1/2}, m_j = 1/2\rangle$  for concreteness. By using a two-photon transition with  $\sigma_+$  polarized 459 nm and  $\pi$  polarized 1038 nm beams, the coherent Rydberg excitation between  $|1\rangle$  and  $|r\rangle$  can be realized where the intermediate state is chosen as  $|p\rangle \equiv |7p_{1/2}, F = 3, m_F = 1\rangle$ . The lifetime of state  $|p\rangle$  and  $|r\rangle$  are  $\tau_p = 0.155 \mu\text{s}$  and  $\tau_r = 592 \mu\text{s}$  un-

der the room temperature (300 K). The branching ratios equal to  $b_{0(1)p} = 1/16$ ,  $b_{dp} = 7/8$ ,  $d_{1(0)r} = 1/32$ ,  $d_{dr} = 7/16$ ,  $d_{pr} = 1/2$ .

In such a structure, we numerically simulated the gate fidelity under the same parameters with  $^{87}\text{Rb}$ , i.e.  $\{\Omega_0, \Omega_2\}/2\pi = \{160, 200\} \text{ MHz}$ . According to the relevant levels of  $^{133}\text{Cs}$ , a 459 nm beam with typical beam power  $P_0 = 402 \mu\text{W}$  and waist of  $\omega_{x|y,0} = 4 \mu\text{m}$  can provide the Rabi frequency  $\Omega_0/2\pi = 160 \text{ MHz}$  of  $|1\rangle \rightarrow |p\rangle$  transition. By tuning the 1038 nm beam with typical beam power  $P_2 = 369 \text{ mW}$  and waist of  $\omega_{x|y,2} = 2 \mu\text{m}$ , we can obtain  $\Omega_2/2\pi = 200 \text{ MHz}$ . The gate fidelity can reach  $\mathcal{F}_t = 0.9981$  with evolution time  $T_g = 0.628 \mu\text{s}$ . Compared with the method provided in Ref. [80], we obtain a higher fidelity with analytic lasers instead of numerical ones.

In addition, this  $C_z$  gate protocol can also be used for the preparation of graph-states as shown in Ref. [63]. Graph state is a kind of quantum entangled state, which can be represented intuitively by graph [102]. Graph state consists of vertices and edges, i.e.  $|G\rangle = (V, E)$ , where each vertex represents a qubit, and each edge represents a correlation. The graph state can be obtained by applying a sequence two-qubit  $C_z$  gate to the empty graph  $|+\rangle^{\otimes n} = [(|0\rangle + |1\rangle)/\sqrt{2}]^{\otimes n}$ , which are important resources for quantum computation and quantum error correction.

#### V. CONCLUSION

We construct a neutral atomic system and generate a  $C_z$  gate under the Rydberg strong blockade situation combined with adiabatic evolution. To reduce the unexpected loss of atoms remaining in the Rydberg state, the control atom and the target atom are driven symmetrically and continuously. By designing a single temporal-modulated Gaussian pulse, states  $|11\rangle$  and  $|10(01)\rangle$  evolve along different adiabatic paths which accumulate a dynamic phase factor of  $\pi$  on logic qubit state  $|11\rangle$  alone at the end of the operation. The method is conductive to create an arbitrary controlled-phase gate. The gate fidelity of the system composed of  $^{87}\text{Rb}$  and  $^{133}\text{Cs}$  atoms can reach  $\mathcal{F}_t = 0.9978, 0.9981$  with operation time less than  $1 \mu\text{s}$ , respectively, considering the dissipation at room temperature. The analytical form of the Gaussian pulse under different pa-

rameters can simply dominate by numerical integration. In addition, we discuss the influences of the technical imperfections under the system composed of  $^{87}\text{Rb}$  atoms. By selecting appropriate optical traps, the predicted gate fidelity can maintain at about 98.4% after correcting the measurement errors. In conclusion, We successfully implemented a fast and high-fidelity  $C_z$  gate in the neutral atomic system. The use of adiabatic pulse reduces the influence of the Doppler effect and laser intensity. Compared with previous methods, our protocol can realize  $C_z$  gate with higher fidelity by using a simple analytic Gaussian pulse and a constant-amplitude pulse. It may be helpful to the experimental implementation of quantum computation and quantum simulation in the neutral-atoms

system.

## ACKNOWLEDGMENT

This work is supported by National Natural Science Foundation of China (NSFC) under Grants No. 11774047 and No. 12174048. W.L. acknowledges support from the EPSRC through Grant No. EP/R04340X/1 via the QuanTERA project “ERyQSenS,” the Royal Society Grant No. IEC\NSFC\181078.

---

[1] Immanuel Bloch, “Quantum coherence and entanglement with ultracold atoms in optical lattices,” *Nature* **453**, 1016–1022 (2008).

[2] M. Saffman, T. G. Walker, and K. Mølmer, “Quantum information with rydberg atoms,” *Rev. Mod. Phys.* **82**, 2313–2363 (2010).

[3] D. Tong, S. M. Farooqi, J. Stanojevic, S. Krishnan, Y. P. Zhang, R. Côté, E. E. Eyler, and P. L. Gould, “Local blockade of rydberg excitation in an ultracold gas,” *Phys. Rev. Lett.* **93**, 063001 (2004).

[4] Kilian Singer, Markus Reetz-Lamour, Thomas Amthor, Luis Gustavo Marcassa, and Matthias Weidemüller, “Suppression of excitation and spectral broadening induced by interactions in a cold gas of rydberg atoms,” *Phys. Rev. Lett.* **93**, 163001 (2004).

[5] T. Cubel Liebisch, A. Reinhard, P. R. Berman, and G. Raithel, “Atom counting statistics in ensembles of interacting rydberg atoms,” *Phys. Rev. Lett.* **95**, 253002 (2005).

[6] E. Urban, T. A. Johnson, T. Henage, L. Isenhower, D. D. Yavuz, T. G. Walker, and M. Saffman, “Observation of rydberg blockade between two atoms,” *Nature Physics* **5**, 110–114 (2009).

[7] Alpha Gaëtan, Yevhen Miroshnychenko, Tatjana Wilk, Amodsen Chotia, Matthieu Viteau, Daniel Comparat, Pierre Pillet, Antoine Browaeys, and Philippe Grangier, “Observation of collective excitation of two individual atoms in the rydberg blockade regime,” *Nature Physics* **5**, 115–118 (2009).

[8] C. Ates, T. Pohl, T. Pattard, and J. M. Rost, “Antiblockade in rydberg excitation of an ultracold lattice gas,” *Phys. Rev. Lett.* **98**, 023002 (2007).

[9] T. Pohl and P. R. Berman, “Breaking the dipole blockade: Nearly resonant dipole interactions in few-atom systems,” *Phys. Rev. Lett.* **102**, 013004 (2009).

[10] Jun Qian, Yong Qian, Min Ke, Xun-Li Feng, C. H. Oh, and Yuzhu Wang, “Breakdown of the dipole blockade with a zero-area phase-jump pulse,” *Phys. Rev. A* **80**, 053413 (2009).

[11] Thomas Amthor, Christian Giese, Christoph S. Hofmann, and Matthias Weidemüller, “Evidence of antiblockade in an ultracold rydberg gas,” *Phys. Rev. Lett.* **104**, 013001 (2010).

[12] J. E. Johnson and S. L. Rolston, “Interactions between rydberg-dressed atoms,” *Phys. Rev. A* **82**, 033412 (2010).

[13] G. Pupillo, A. Micheli, M. Boninsegni, I. Lesanovsky, and P. Zoller, “Strongly correlated gases of rydberg-dressed atoms: Quantum and classical dynamics,” *Phys. Rev. Lett.* **104**, 223002 (2010).

[14] T. Macrì and T. Pohl, “Rydberg dressing of atoms in optical lattices,” *Phys. Rev. A* **89**, 011402 (2014).

[15] J B Balewski, A T Krupp, A Gaj, S Hofferberth, R Löw, and T Pfau, “Rydberg dressing: understanding of collective many-body effects and implications for experiments,” *New Journal of Physics* **16**, 063012 (2014).

[16] Michael J. Martin, Yuan-Yu Jau, Jongmin Lee, Anupam Mitra, Ivan H. Deutsch, and Grant W. Biedermann, “A mølmer-sørensen gate with rydberg-dressed atoms,” (2021), [arXiv:2111.14677 \[quant-ph\]](https://arxiv.org/abs/2111.14677).

[17] M Saffman, “Quantum computing with atomic qubits and rydberg interactions: progress and challenges,” *Journal of Physics B: Atomic, Molecular and Optical Physics* **49**, 202001 (2016).

[18] D. Jaksch, J. I. Cirac, P. Zoller, S. L. Rolston, R. Côté, and M. D. Lukin, “Fast quantum gates for neutral atoms,” *Phys. Rev. Lett.* **85**, 2208–2211 (2000).

[19] M. D. Lukin, M. Fleischhauer, R. Cote, L. M. Duan, D. Jaksch, J. I. Cirac, and P. Zoller, “Dipole blockade and quantum information processing in mesoscopic atomic ensembles,” *Phys. Rev. Lett.* **87**, 037901 (2001).

[20] E Brion, L H Pedersen, and K Mølmer, “Implementing a neutral atom rydberg gate without populating the rydberg state,” *Journal of Physics B: Atomic, Molecular and Optical Physics* **40**, S159–S166 (2007).

[21] E. Brion, A. S. Mouritzen, and K. Mølmer, “Conditional dynamics induced by new configurations for rydberg dipole-dipole interactions,” *Phys. Rev. A* **76**, 022334 (2007).

[22] Huai-Zhi Wu, Zhen-Biao Yang, and Shi-Biao Zheng, “Implementation of a multiqubit quantum phase gate in a neutral atomic ensemble via the asymmetric rydberg blockade,” *Phys. Rev. A* **82**, 034307 (2010).

[23] M. M. Müller, D. M. Reich, M. Murphy, H. Yuan, J. Vala, K. B. Whaley, T. Calarco, and C. P. Koch, “Optimizing entangling quantum gates for physical systems,” *Phys. Rev. A* **84**, 042315 (2011).

[24] T. Xia, X. L. Zhang, and M. Saffman, “Analysis of a controlled phase gate using circular rydberg states,” *Phys. Rev. A* **88**, 062337 (2013).

[25] L. S. Theis, F. Motzoi, F. K. Wilhelm, and M. Saffman, “High-fidelity rydberg-blockade entangling gate using shaped, analytic pulses,” *Phys. Rev. A* **94**, 032306 (2016).

[26] David Petrosyan, Felix Motzoi, Mark Saffman, and Klaus Mølmer, “High-fidelity rydberg quantum gate via a two-atom dark state,” *Phys. Rev. A* **96**, 042306 (2017).

[27] Xiao-Feng Shi, “Deutsch, toffoli, and cnot gates via rydberg blockade of neutral atoms,” *Phys. Rev. Applied* **9**, 051001 (2018).

[28] Xi-Rong Huang, Zong-Xing Ding, Chang-Sheng Hu, Li-Tuo Shen, Weibin Li, Huaizhi Wu, and Shi-Biao Zheng, “Robust rydberg gate via landau-zener control of förster resonance,” *Phys. Rev. A* **98**, 052324 (2018).

[29] A. W. Carr and M. Saffman, “Preparation of entangled and antiferromagnetic states by dissipative rydberg pumping,” *Phys. Rev. Lett.* **111**, 033607 (2013).

[30] Xiao-Feng Shi, “Hyperentanglement of divalent neutral atoms by rydberg blockade,” *Phys. Rev. A* **104**, 042422 (2021).

[31] Lőrinc Sárkány, József Fortágh, and David Petrosyan, “Long-range quantum gate via rydberg states of atoms in a thermal microwave cavity,” *Phys. Rev. A* **92**, 030303 (2015).

[32] Shi-Lei Su, Erjun Liang, Shou Zhang, Jing-Ji Wen, Li-Li Sun, Zhao Jin, and Ai-Dong Zhu, “One-step implementation of the rydberg-rydberg-interaction gate,” *Phys. Rev. A* **93**, 012306 (2016).

[33] Shi-Lei Su, Ya Gao, Erjun Liang, and Shou Zhang, “Fast rydberg antiblockade regime and its applications in quantum logic gates,” *Phys. Rev. A* **95**, 022319 (2017).

[34] Matteo Marcuzzi, Jiří Minář, Daniel Barredo, Sylvain de Léséleuc, Henning Labuhn, Thierry Lahaye, Antoine Browaeys, Emanuele Levi, and Igor Lesanovsky, “Facilitation dynamics and localization phenomena in rydberg lattice gases with position disorder,” *Phys. Rev. Lett.* **118**, 063606 (2017).

[35] S. L. Su, H. Z. Shen, Erjun Liang, and Shou Zhang, “One-step construction of the multiple-qubit rydberg controlled-phase gate,” *Phys. Rev. A* **98**, 032306 (2018).

[36] Maike Ostmann, Matteo Marcuzzi, Juan P. Garrahan, and Igor Lesanovsky, “Localization in spin chains with facilitation constraints and disordered interactions,” *Phys. Rev. A* **99**, 060101 (2019).

[37] Paolo P. Mazza, Richard Schmidt, and Igor Lesanovsky, “Vibrational dressing in kinetically constrained rydberg spin systems,” *Phys. Rev. Lett.* **125**, 033602 (2020).

[38] Jin-Lei Wu, Yan Wang, Jin-Xuan Han, Shi-Lei Su, Yan Xia, Yongyuan Jiang, and Jie Song, “Resilient quantum gates on periodically driven rydberg atoms,” *Phys. Rev. A* **103**, 012601 (2021).

[39] David Petrosyan and Klaus Mølmer, “Binding potentials and interaction gates between microwave-dressed rydberg atoms,” *Phys. Rev. Lett.* **113**, 123003 (2014).

[40] Tyler Keating, Robert L. Cook, Aaron M. Hankin, Yuan-Yu Jau, Grant W. Biedermann, and Ivan H. Deutsch, “Robust quantum logic in neutral atoms via adiabatic rydberg dressing,” *Phys. Rev. A* **91**, 012337 (2015).

[41] Y.-Y. Jau, A. M. Hankin, T. Keating, I. H. Deutsch, and G. W. Biedermann, “Entangling atomic spins with a rydberg-dressed spin-flip blockade,” *Nature Physics* **12**, 71–74 (2016).

[42] Xiao-Feng Shi and T. A. B. Kennedy, “Annulled van der waals interaction and fast rydberg quantum gates,” *Phys. Rev. A* **95**, 043429 (2017).

[43] Anupam Mitra, Michael J. Martin, Grant W. Biedermann, Alberto M. Marino, Pablo M. Poggi, and Ivan H. Deutsch, “Robust mølmer-sørensen gate for neutral atoms using rapid adiabatic rydberg dressing,” *Phys. Rev. A* **101**, 030301 (2020).

[44] Jeremy T. Young, Przemyslaw Bienias, Ron Belyansky, Adam M. Kaufman, and Alexey V. Gorshkov, “Asymmetric blockade and multiqubit gates via dipole-dipole interactions,” *Phys. Rev. Lett.* **127**, 120501 (2021).

[45] Rui Han, Hui Khoon Ng, and Berthold-Georg Englert, “Implementing a neutral-atom controlled-phase gate with a single rydberg pulse,” *EPL (Europhysics Letters)* **113**, 40001 (2016).

[46] Xiao-Feng Shi, “Fast, accurate, and realizable two-qubit entangling gates by quantum interference in detuned rabi cycles of rydberg atoms,” *Phys. Rev. Applied* **11**, 044035 (2019).

[47] Xiao-Feng Shi, “Rydberg quantum gates free from blockade error,” *Phys. Rev. Applied* **7**, 064017 (2017).

[48] T. H. Xing, P. Z. Zhao, and D. M. Tong, “Realization of nonadiabatic holonomic multiqubit controlled gates with rydberg atoms,” *Phys. Rev. A* **104**, 012618 (2021).

[49] Xiao-Feng Shi and Yan Lu, “Quantum gates with weak van der waals interactions of neutral rydberg atoms,” *Phys. Rev. A* **104**, 012615 (2021).

[50] Nathan Schine, Aaron W. Young, William J. Eckner, Michael J. Martin, and Adam M. Kaufman, “Long-lived bell states in an array of optical clock qubits,” (2021), [arXiv:2111.14653 \[physics.atom-ph\]](https://arxiv.org/abs/2111.14653).

[51] Yucheng He, Jing-Xin Liu, F. Q. Guo, Lei-Lei Yan, Ronghui Luo, Erjun Liang, Shi-Lei Su, and M. Feng, “Multiple-qubit rydberg quantum logic gate via dressed-states scheme,” (2021), [arXiv:2010.14704 \[quant-ph\]](https://arxiv.org/abs/2010.14704).

[52] M. Saffman and T. G. Walker, “Analysis of a quantum logic device based on dipole-dipole interactions of optically trapped rydberg atoms,” *Phys. Rev. A* **72**, 022347 (2005).

[53] L. Isenhower, E. Urban, X. L. Zhang, A. T. Gill, T. Henage, T. A. Johnson, T. G. Walker, and M. Saffman, “Demonstration of a neutral atom controlled-not quantum gate,” *Phys. Rev. Lett.* **104**, 010503 (2010).

[54] T. Wilk, A. Gaëtan, C. Evellin, J. Wolters, Y. Miroshnychenko, P. Grangier, and A. Browaeys, “Entanglement of two individual neutral atoms using rydberg blockade,” *Phys. Rev. Lett.* **104**, 010502 (2010).

[55] X. L. Zhang, L. Isenhower, A. T. Gill, T. G. Walker, and M. Saffman, “Deterministic entanglement of two neutral atoms via rydberg blockade,” *Phys. Rev. A* **82**, 030306 (2010).

[56] X. L. Zhang, A. T. Gill, L. Isenhower, T. G. Walker, and M. Saffman, “Fidelity of a rydberg-blockade quantum gate from simulated quantum process tomography,” *Phys. Rev. A* **85**, 042310 (2012).

[57] K. M. Maller, M. T. Lichtman, T. Xia, Y. Sun, M. J. Piotrowicz, A. W. Carr, L. Isenhower, and M. Saffman, “Rydberg-blockade controlled-not gate and entanglement in a two-dimensional array of neutral-atom qubits,” *Phys. Rev. A* **92**, 022336 (2015).

[58] T. M. Graham, M. Kwon, B. Grinkemeyer, Z. Marra, X. Jiang, M. T. Lichtman, Y. Sun, M. Ebert, and M. Saffman, “Rydberg-mediated entanglement in a two-dimensional neutral atom qubit array,” *Phys. Rev. Lett.* **123**, 230501 (2019).

[59] Harry Levine, Alexander Keesling, Ahmed Omran, Hannes Bernien, Sylvain Schwartz, Alexander S. Zibrov, Manuel Endres, Markus Greiner, Vladan Vuletić, and Mikhail D. Lukin, “High-fidelity control and entanglement of rydberg-atom qubits,” *Phys. Rev. Lett.* **121**, 123603 (2018).

[60] Harry Levine, Alexander Keesling, Giulia Semeghini, Ahmed Omran, Tout T. Wang, Sepehr Ebadi, Hannes Bernien, Markus Greiner, Vladan Vuletić, Hannes Pichler, and Mikhail D. Lukin, “Parallel implementation of high-fidelity multiqubit gates with neutral atoms,” *Phys. Rev. Lett.* **123**, 170503 (2019).

[61] Yuan Sun, Peng Xu, Ping-Xing Chen, and Liang Liu, “Controlled phase gate protocol for neutral atoms via off-resonant modulated driving,” *Phys. Rev. Applied* **13**, 024059 (2020).

[62] Yangyang Liu, Yuan Sun, Zhuo Fu, Peng Xu, Xin Wang, Xiaodong He, Jin Wang, and Mingsheng Zhan, “Infidelity induced by ground-rydberg decoherence of the control qubit in

a two-qubit rydberg-blockade gate,” *Phys. Rev. Applied* **15**, 054020 (2021).

[63] Dolev Bluvstein, Harry Levine, Giulia Semeghini, Tout T. Wang, Sepehr Ebadi, Marcin Kalinowski, Alexander Keesling, Nishad Maskara, Hannes Pichler, Markus Greiner, Vladan Vuletic, and Mikhail D. Lukin, “A quantum processor based on coherent transport of entangled atom arrays,” (2021), [arXiv:2112.03923 \[quant-ph\]](https://arxiv.org/abs/2112.03923).

[64] Zhuo Fu, Peng Xu, Yuan Sun, Yangyang Liu, Xiaodong He, Xiao Li, Min Liu, Runbing Li, Jin Wang, Liang Liu, and Mingsheng Zhan, “High fidelity entanglement of neutral atoms via a rydberg-mediated single-modulated-pulse controlled-phase gate,” (2021), [arXiv:2109.02491 \[quant-ph\]](https://arxiv.org/abs/2109.02491).

[65] Rui Li, Shurui Li, Dongmin Yu, Jing Qian, and Weiping Zhang, “Optimal model for fewer-qubit cnot gates with rydberg atoms,” (2021), [arXiv:2112.08747 \[quant-ph\]](https://arxiv.org/abs/2112.08747).

[66] Michael H. Goerz, Eli J. Halperin, Jon M. Aytac, Christiane P. Koch, and K. Birgitta Whaley, “Robustness of high-fidelity rydberg gates with single-site addressability,” *Phys. Rev. A* **90**, 032329 (2014).

[67] J. F. Haase, Z.-Y. Wang, J. Casanova, and M. B. Plenio, “Soft quantum control for highly selective interactions among joint quantum systems,” *Phys. Rev. Lett.* **121**, 050402 (2018).

[68] Hong-Da Yin and Xiao-Qiang Shao, “Gaussian soft control-based quantum fan-out gate in ground-state manifolds of neutral atoms,” *Opt. Lett.* **46**, 2541–2544 (2021).

[69] Li-Na Sun, L.-L. Yan, Shi-Lei Su, and Y. Jia, “One-step implementation of time-optimal-control three-qubit nonadiabatic holonomic controlled gates in rydberg atoms,” *Phys. Rev. Applied* **16**, 064040 (2021).

[70] Edward Farhi, Jeffrey Goldstone, Sam Gutmann, Joshua Lapan, Andrew Lundgren, and Daniel Pread, “A quantum adiabatic evolution algorithm applied to random instances of an np-complete problem,” *Science* **292**, 472–475 (2001).

[71] Ditte Møller, Lars Bojer Madsen, and Klaus Mølmer, “Quantum gates and multiparticle entanglement by rydberg excitation blockade and adiabatic passage,” *Phys. Rev. Lett.* **100**, 170504 (2008).

[72] Matthias M. Müller, Harald R. Haakh, Tommaso Calarco, Christiane P. Koch, and Carsten Henkel, “Prospects for fast rydberg gates on an atom chip,” *Quantum Information Processing* **10**, 771 (2011).

[73] Matthias M. Müller, Michael Murphy, Simone Montangero, Tommaso Calarco, Philippe Grangier, and Antoine Browaeys, “Implementation of an experimentally feasible controlled-phase gate on two blockaded rydberg atoms,” *Phys. Rev. A* **89**, 032334 (2014).

[74] Yuan Sun and Harold Metcalf, “Nonadiabaticity in stimulated raman adiabatic passage,” *Phys. Rev. A* **90**, 033408 (2014).

[75] Yan Liang, Qi-Cheng Wu, Shi-Lei Su, Xin Ji, and Shou Zhang, “Shortcuts to adiabatic passage for multiqubit controlled-phase gate,” *Phys. Rev. A* **91**, 032304 (2015).

[76] I. I. Beterov, M. Saffman, E. A. Yakshina, D. B. Tretyakov, V. M. Entin, S. Bergamini, E. A. Kuznetsova, and I. I. Ryabtsev, “Two-qubit gates using adiabatic passage of the stark-tuned förster resonances in rydberg atoms,” *Phys. Rev. A* **94**, 062307 (2016).

[77] D. D. Bhaktavatsala Rao and Klaus Mølmer, “Robust rydberg-interaction gates with adiabatic passage,” *Phys. Rev. A* **89**, 030301 (2014).

[78] Huaizhi Wu, Xi-Rong Huang, Chang-Sheng Hu, Zhen-Biao Yang, and Shi-Biao Zheng, “Rydberg-interaction gates via adiabatic passage and phase control of driving fields,” *Phys. Rev. A* **96**, 022321 (2017).

[79] I. I. Beterov, G. N. Hamzina, E. A. Yakshina, D. B. Tretyakov, V. M. Entin, and I. I. Ryabtsev, “Adiabatic passage of radio-frequency-assisted förster resonances in rydberg atoms for two-qubit gates and the generation of bell states,” *Phys. Rev. A* **97**, 032701 (2018).

[80] M. Saffman, I. I. Beterov, A. Dalal, E. J. Páez, and B. C. Sanders, “Symmetric rydberg controlled- $z$  gates with adiabatic pulses,” *Phys. Rev. A* **101**, 062309 (2020).

[81] Meng Li, F.-Q. Guo, Z. Jin, L.-L. Yan, E.-J. Liang, and S.-L. Su, “Multiple-qubit controlled unitary quantum gate for rydberg atoms using shortcut to adiabaticity and optimized geometric quantum operations,” *Phys. Rev. A* **103**, 062607 (2021).

[82] Chi Zhang, Fabian Pokorny, Weibin Li, Gerard Higgins, Andreas Pöschl, Igor Lesanovsky, and Markus Hennrich, “Submicrosecond entangling gate between trapped ions via rydberg interaction,” *Nature* **580**, 345–349 (2020).

[83] F. Robicheaux, T. M. Graham, and M. Saffman, “Photon-recoil and laser-focusing limits to rydberg gate fidelity,” *Phys. Rev. A* **103**, 022424 (2021).

[84] Adriano Barenco, David Deutsch, Artur Ekert, and Richard Jozsa, “Conditional quantum dynamics and logic gates,” *Phys. Rev. Lett.* **74**, 4083–4086 (1995).

[85] A. Galindo and M. A. Martín-Delgado, “Information and computation: Classical and quantum aspects,” *Rev. Mod. Phys.* **74**, 347–423 (2002).

[86] N. Šibalić, J.D. Pritchard, C.S. Adams, and K.J. Weatherill, “Arc: An open-source library for calculating properties of alkali rydberg atoms,” *Computer Physics Communications* **220**, 319–331 (2017).

[87] M. P. Fewell, B. W. Shore, and K. Bergmann, “Coherent population transfer among three states: full algebraic solutions and the relevance of non adiabatic processes to transfer by delayed pulses,” *Australian Journal of Physics* **50**, 281–308 (1997).

[88] B. W. Shore, *The Theory of Coherent Atomic Excitation*. (1990).

[89] J. F. Barry, D. J. McCarron, E. B. Norrgard, M. H. Steinecker, and D. DeMille, “Magneto-optical trapping of a diatomic molecule,” *Nature* **512**, 286–289 (2014).

[90] Jiazhong Hu, Alban Urvoy, Zachary Vendeiro, Valentin Crépel, Wenlan Chen, and Vladan Vuletić, “Creation of a bose-condensed gas of  $^{87}\text{rb}$  by laser cooling,” *Science* **358**, 1078–1080 (2017).

[91] R V Brooks, S Spence, A Guttridge, A Alampouli, A Rakonjac, L A McARD, Jeremy M Hutson, and Simon L Cornish, “Preparation of one  $^{87}\text{rb}$  and one  $^{133}\text{Cs}$  atom in a single optical tweezer,” *New Journal of Physics* **23**, 065002 (2021).

[92] A. M. Kaufman, B. J. Lester, and C. A. Regal, “Cooling a single atom in an optical tweezer to its quantum ground state,” *Phys. Rev. X* **2**, 041014 (2012).

[93] C. Tuchendler, A. M. Lance, A. Browaeys, Y. R. P. Sortais, and P. Grangier, “Energy distribution and cooling of a single atom in an optical tweezer,” *Phys. Rev. A* **78**, 033425 (2008).

[94] Rudolf Grimm, Matthias Weidmüller, and Yurii B. Ovchinnikov, “Optical dipole traps for neutral atoms,” in *Advances in Atomic, Molecular, and Optical Physics*, Advances In Atomic, Molecular, and Optical Physics, Vol. 42, edited by Benjamin Bederson and Herbert Walther (Academic Press, 2000) pp. 95–170.

[95] Thad G. Walker and Mark Saffman, “Chapter 2 - entanglement of two atoms using rydberg blockade,” in *Advances in Atomic, Molecular, and Optical Physics*, Advances In Atomic, Molecular, and Optical Physics, Vol. 61, edited by Paul Berman, Ennio Arimondo, and Chun Lin (Academic Press, 2012) pp. 81–

115.

[96] Hikaru Tamura, Tomotake Yamakoshi, and Ken'ichi Nakagawa, "Analysis of coherent dynamics of a rydberg-atom quantum simulator," *Phys. Rev. A* **101**, 043421 (2020).

[97] Xiao-Feng Shi, "Suppressing motional dephasing of ground-rydberg transition for high-fidelity quantum control with neutral atoms," *Phys. Rev. Applied* **13**, 024008 (2020).

[98] Katharina Gillen-Christandl, Glen D. Gillen, M. J. Piotrowicz, and M Saffman, "Comparison of gaussian and super gaussian laser beams for addressing atomic qubits," *Applied Physics B* **122**, 131 (2016).

[99] Sylvain de Léséleuc, Daniel Barredo, Vincent Lienhard, Antoine Browaeys, and Thierry Lahaye, "Analysis of imperfections in the coherent optical excitation of single atoms to rydberg states," *Phys. Rev. A* **97**, 053803 (2018).

[100] Woojun Lee, Minhyuk Kim, Hanlae Jo, Yunheung Song, and Jaewook Ahn, "Coherent and dissipative dynamics of entangled few-body systems of rydberg atoms," *Phys. Rev. A* **99**, 043404 (2019).

[101] A. M. Hankin, Y.-Y. Jau, L. P. Parazzoli, C. W. Chou, D. J. Armstrong, A. J. Landahl, and G. W. Biedermann, "Two-atom rydberg blockade using direct  $6s$  to  $np$  excitation," *Phys. Rev. A* **89**, 033416 (2014).

[102] M. Hein, J. Eisert, and H. J. Briegel, "Multiparty entanglement in graph states," *Phys. Rev. A* **69**, 062311 (2004).